Full length article

A CRTH2 antagonist, CT-133, suppresses NF-κB signalling to relieve lipopolysaccharide-induced acute lung injury

Musaddique Hussain[a], Chengyun Xu[a,b], Xiling Wu[c], Meiping Lu[c], Lanfang Tang[c], Fugen Wu[d], Ximei Wu[a], Junsong Wu[b,*]

[a] Department of Pharmacology, Zhejiang University, School of Medicine, Hangzhou City, 310058, China
[b] Department of Critical Care Medicine and Orthopedics, The First Affiliated Hospital, Zhejiang University, School of Medicine, Hangzhou City, 310009, China
[c] Department of Respiratory Medicine, The Affiliated Children Hospital, Zhejiang University School of Medicine, Hangzhou City, 310052, China
[d] Department of Pediatrics, The First People's Hospital of Wenling City, Wenling City, 317500, China

A B S T R A C T

Acute lung injury (ALI) and acute respiratory distress syndrome are life-threatening conditions that still have no definite pharmacotherapy. Hence, we investigate the potential effectiveness and underlying mechanism of CT-133, a newly developed selective antagonist of prostaglandin D2 receptor 2 (DP2) or of chemoattractant receptor homologous molecule expressed on Th2 cells (CRTH2), against lipopolysaccharide (LPS)-induced ALI. CT-133 (10 or 30 mg/kg) or dexamethasone (1 mg/kg, positive control) were intragastrically administered 1 h before and 12 h after intratracheal LPS instillation, and primary neutrophils and macrophages and RAW264.7 macrophages were used to investigate the role of CT-133 in regulation of their functions. LPS induced a significant secretion of PGD_2 from primary macrophages, however, CT-133 dose-dependently and markedly decreased the infiltration of neutrophils and macrophages into lungs, reduced the IL-1β, TNF-α, IL-6, and KC levels in bronchoalveolar lavage (BAL) fluids, decreased the wet weight and myeloperoxidase activity of lungs, reduced Evans blue and albumin exudation into lungs, and improved the lung histopathological changes and hypoxemia. Moreover, CT-133 significantly suppressed the primary neutrophil migration toward the PGD_2 and robustly inhibited the mRNA and protein expression of IL-1β, TNF-α, IL-6, and KC in primary and RAW264.7 macrophages in response to either LPS- or PGD_2 stimulation. Finally, CT-133 significantly blocked the LPS-induced P65 activation in both RAW264.7 macrophages and mouse lungs. Thus, This is the first report that a CRTH2 antagonist, CT-133, is capable of significantly alleviating LPS-induced lung injury by probably down-regulating the NF-κB signalling.

1. Introduction

Acute lung injury (ALI) and acute respiratory distress syndrome (ARDS), a more severe form of ALI, are devastating clinical syndromes characterised by alveolar-capillary membrane hyper-permeability, oedema, infiltration of neutrophils into interstitial spaces, neutrophil-derived inflammation, and dysfunction of surfactant and involved cells, including endothelial cells, epithelial cells and macrophages (Wheeler and Bernard, 2007). A recent global observational study revealed increased mortality in patients with ALI/ARDS (Bellani et al., 2016), while surviving patients are at high risk of depression, cognitive decline, persistent skeletal-muscle weakness and post-traumatic stress disorder (Herridge et al., 2016). Despite decades of widespread

research, no distinct pharmacological agent is presently available to manage ALI (Hussain et al., 2018). Therefore, novel pharmacological approaches are urgently needed.

ALI can be induced experimentally by lipopolysaccharide (LPS), a ligand of Toll-like receptor 4 (TLR4) and the primary stimulus of macrophage activation. LPS treatment immediately activates the TLR4-linked nuclear factor kappa-B (NF-κB) signalling pathway (Yang et al., 2017). Generally, NF-κB, a heterodimer composed primarily of P65 and P50, stays in the cytoplasm as an inactive form due to the action of an inhibitory protein IκB, especially IκBα (Karin, 1999; Karin and Ben-Neriah, 2000). Upon inflammatory stimuli such as LPS, IκB is phosphorylated by IκB kinase (IKK) and degraded, thereby releasing NF-κB to translocate into the nucleus, where NF-κB induces the transcription

of several pro-inflammatory cytokines, such as tumour necrosis factor-α (TNF-α), interleukin-1β (IL-1β), IL-6, IL-8, and other inflammatory mediators, such as prostaglandin (PG) D_2/E_2 and nitric oxide (NO) (Bhatia and Moochhala, 2004; Matthay et al., 2012). LPS also stimulates macrophage migration via the chemoattractants PGD_2 and PGE_2 (Tajima et al., 2008) that orchestrate neutrophilic infiltration into the lung (Dhaliwal et al., 2012). The activated neutrophils provoke further lung inflammation (Li et al., 2016; Zhou et al., 2011). Accumulated evidence now indicates that targeting of NF-κB not only alleviates the pro-inflammatory cytokine production but also suppresses the pulmonary oedema and influx of neutrophils, which are key characteristics of ALI (Everhart et al., 2006; Yang et al., 2012). Therefore, LPS-induced ALI mouse models are appropriate for the evaluation of pharmacological effects of therapeutic compounds, because the lung injury symptoms observed in LPS-induced ALI mice overall are consistent with those observed in patients with ARDS.

Emerging evidence reveals that PGD_2, which is mainly produced from allergen-stimulated mast cells and Th2 lymphocytes, has a crucial role in mediating airway inflammation. PGD_2 has diverse functions, including activation of the D-type prostanoid receptors (DPs) DP_1 and DP_2, DP2 is also known as chemoattractant receptor-homologous molecules expressed on Th2 (CRTH2) cells. Activation of PGD_2/CRTH2 receptors on macrophages promotes neutrophil migration and their survival in the lung, as well as augmenting the disease severity through excessive production of pro-inflammatory cytokines and subsequent neutrophil activation. Consequently, antagonism of CRTH2 ameliorates the alveolar influx of neutrophils, thereby lessening the disease severity (Jandl et al., 2016). Furthermore, CRTH2-knockout mice have shown an increased survival rate and decreased levels of pro-inflammatory cytokines and total protein in the lungs in response to LPS injection when compared to control mice (Suzuki et al., 2016). CRTH2 antagonists have been effective in treating eosinophilic esophagitis (Straumann et al., 2013), allergic rhinitis (Krug et al., 2014) and asthma (Gonem et al., 2016; Singh et al., 2013).

These evidence prompted us to investigate the effectiveness of CT-133, a newly discovered, well-tolerated, selective and potent CRTH2 antagonist, as a treatment of ALI. CT-133 has shown a potential response in treating chronic obstructive pulmonary disease (COPD), allergic rhinitis and asthma (Guo, 2015), but it has not been evaluated in LPS-induced ALI models. The present study was designed to explore the protective role of CT-133 in an LPS-induced mouse ALI model and demonstrated that CT-133, a CRTH2 antagonist, suppresses NF-κB signalling to relieve LPS-induced ALI.

2. Materials and methods

2.1. Chemicals and solutions

CT-133 ($C_{20}H_{19}FN_3NaO_4S$), a potent CRTH2 receptor antagonist, with 99.6% purity was obtained from CSPC Pharmaceutical Group (Shijiazhuang City, China) (Hussain et al., 2019). The pharmacological features of CT-133 have been previously reported (Guo, 2015; Hussain et al., 2019). Briefly, CT-133 showed potent human CRTH2 inhibition with inhibitory constant (Ki) of 2.2 nM whereas the inhibitory constant (Ki) for Human DP1 was > 3800 nM. All chemicals were of research grade. Lipopolysaccharide (LPS; *Escherichia coli* O127: B8), dexamethasone (Dex), phosphate buffered saline (PBS), penicillin, fetal bovine serum (FBS) and Evans blue dye (EBD) were purchased from Sigma Chemical Co. (St. Louis, MO, USA). TNF-α, IL-1β, IL-6 and keratinocyte chemoattractant (KC) ELISA kits were obtained from Multisciences Biotech Ltd. (Hangzhou, China). Albumin and MPO determination kits were bought from Jiancheng Bioengineering Institute of Nanjing (Nanjing, China). TNF-α, IL-1β, IL-6, KC and β-actin PCR primers were purchased from Shanghai Bioengineering Ltd. (Shanghai, China). Roswell Park Memorial Institute (RPMI) 1640 medium and high glucose of Dulbecco's modification of Eagle's (DMEM) medium were

obtained from GE Healthcare Life Sciences (Pittsburgh, PA). Prostaglandin D_2 (PGD_2) and PGD_2 ELISA kit were purchased from Cayman chemical (Ann Arbor, MI). RNAiso plus was obtained from Takara Bio Inc. (Otsu, Shiga, Japan). HiScript $5 \times Q$ RT Super Mix, including buffer, dNTP, HiScript Reverse Transcriptase, RNase inhibitor, and Random primers/Oligo dT primer mix, and SYBR Green Master Mix were obtained from Vazyme Biotech, Ltd. (Nanjing, China). Mouse or rabbit antibodies specific to IκBα, phospho-IκBα, P65, phospho-P65 were purchased from Cell Signalling Technology (Danvers, MA) while β-actin was Santa Cruz Biotechnology (Santa Cruz, CA). Secondary antibodies IRDye 680 and 800 were purchased from LI-COR Biosciences (Lincoln, Nebraska). CT-133 solutions at 10 and 30 mg/kg and Dex suspension at 1 mg/kg were prepared by dissolving an appropriate amount of respective drug in 0.9% normal saline, and all prepared solutions were kept in a dark place at 4 °C for no more than one week. The administration volume for each mouse was 10 ml/kg body weight.

2.2. Mice handling, preparation of LPS-induced ALI models, and measurement of oxygen saturation

Specific pathogen-free (SPF) Balb/c mice (♂/♀, 8 weeks old, 20–26 g) were purchased from Shanghai SIPPR-BK Laboratory Animals Co. Ltd. Shanghai, China (certificate No. SCK (hu) 2013–0016 and 2008001648391). Mice were housed under controlled environmental conditions (24 ± 2 °C; 50 ± 10% humidity) with 12 h/12 h dark-light cycle and had free access to distilled water and regular rodent chow. Institutional Animal Care and Use Committee of Zhejiang University accomplished all animal care and handling procedures. LPS-induced ALI models were prepared as previously described with slight modification (Zhang et al., 2017). In brief, mice were randomly divided into control group (12 mice) and LPS group (48 mice) while LPS group was further divided into four subgroups (each group contained 12 mice). For acute lung injury, unanesthetized mice of LPS group received intragastric administration of normal saline (NS), CT-133 at 10 or 30 mg/kg and Dex at 1 mg/kg, respectively. One hour later, mice were anesthetized with sodium pentobarbital (intraperitoneal injection at 40 mg/kg) and then subjected to intratracheal instillation of NS to control group and LPS (4 mg/kg) to all LPS subgroups. Twelve hours after LPS instillation, unanesthetized mice of LPS group were intragastrically administrated with NS, CT-133 at 10 or 30 mg/kg and Dex at 1 mg/kg, respectively (Fig. 1). Both normal saline and LPS were administered at 10 μl/10 g of body weight. Twenty-four hours after LPS challenge, the oxygen saturation (SO_2) of all mice was measured by using the moor VMS-OXY™ monitor (Moor Instruments, Devon, UK) which measures SO_2 (%) in the microcirculation at the wavelength range of 500–650 nm. SO_2 represents the percentage of oxygenated hemoglobin in the blood to total hemoglobin. After measurement of SO_2, BAL fluid from each mouse was collected for inflammatory cell counting and classification and for determination of albumin concentration and pro-inflammatory cytokines/chemokine levels, whereas lung was subjected for determination of weight coefficient and of MPO activity as well as histological examination.

2.3. Cells counting and lung weight coefficient

Mice were killed to surgically expose the trachea, and then right lungs were lavaged with 0.4 ml/time of sterilized NS containing 1% bovine serum albumin (BSA) and 5000 IU/L heparin three times to collect the BAL fluid via tracheal tube. After counting the total inflammatory cells in BAL fluid with a hemocytometer, remainder BAL fluid was centrifuged immediately at $1000 \times g$ at 4 °C for 10 min. The supernatant was aliquoted and stored at −80 °C until measurement of pro-inflammatory cytokines or albumin concentration. Obtained cell pellets were smeared on slides. Afterward, Wright-Giemsa staining of prepared smears was performed to count 200 cells under a light microscope according to the morphological criteria of neutrophils,
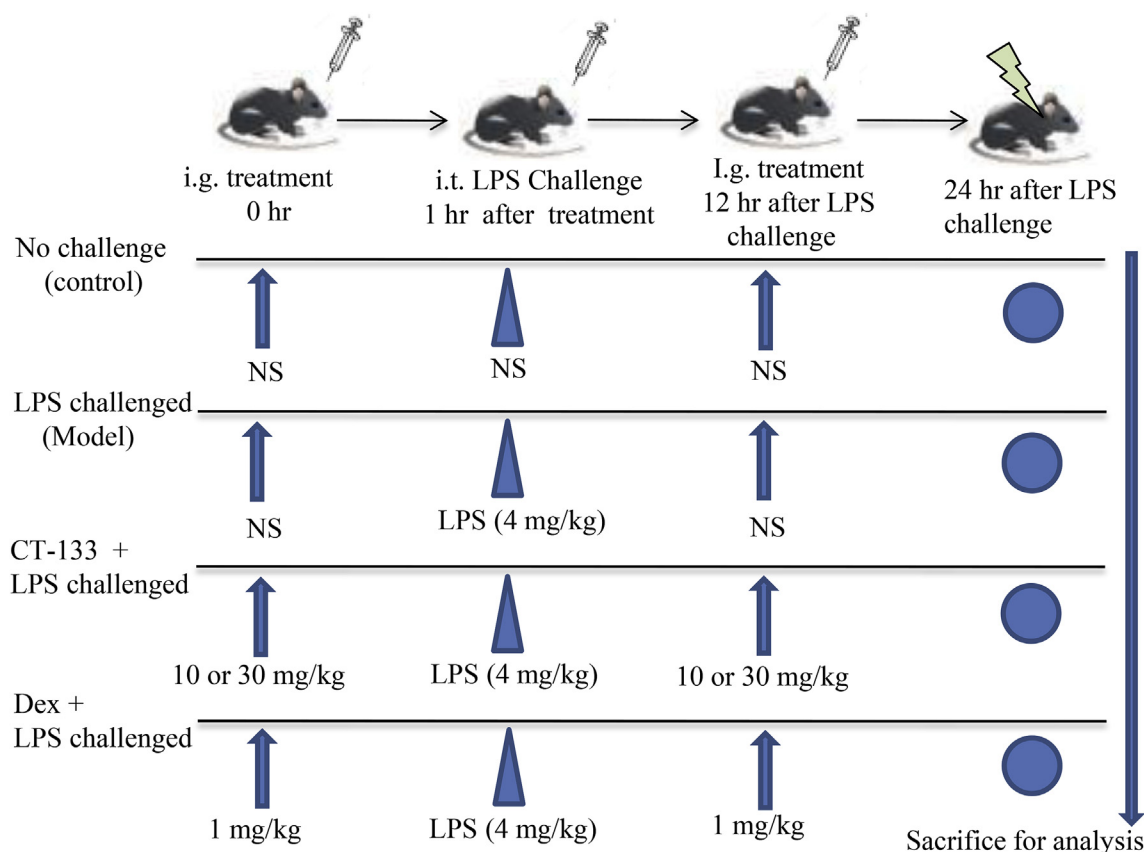
Fig. 1. A schematic sketch showing the procedure for preparing the LPS-induced ALI mouse model. CT-133 (10 and 30 mg/kg) or Dex (positive control; 1 mg/kg) were intragastrically administered 1 h before and 12 h after intratracheal LPS instillation. Twenty-four hours after the LPS challenge, Mice were sacrificed for preparation of BAL fluids and lung tissue samples.

macrophage, and lymphocyte. Removed lung tissues were weighted after aspirating the surface blood and then lung weight coefficient, an indicator of pulmonary oedema, was measured by dividing the individual lung weight of each mouse by its total body weight.

2.4. In vivo pro-inflammatory cytokines and chemokine assessment via ELISA

Expression levels of pro-inflammatory cytokines (IL-β, TNF-α, IL-6) and chemokine (KC; mouse homologue of IL-8) in the BAL fluid were assessed by using respective ELISA determination kits according to the manufacturer's instructions. After measurements of the optical density at 450 nm, expression of contents was calculated via standard curves.

2.5. Histological examination

For histological examination, lower lobe of the left lung of each mouse was inflated with neutral buffered 10% formalin instilled at room temperature under constant pressure of 22–25 cm H_2O for 48 h. Inflated lobes were embedded in paraffin and then sectioned (4 μm) to expose the maximum longitudinal view of the main intrapulmonary bronchus. Afterward, hematoxylin-eosin (H&E) staining was accomplished to evaluate the lung oedema and infiltration of neutrophils and inflammatory cells under the light microscopy. The severity of lung injury was measured by slightly modifying the previously described scoring system (Matute-Bello et al., 2011; Mrozek et al., 1997). Briefly, lung oedema, haemorrhage, alveolar wall thickening and infiltration of neutrophils and inflammatory cells were counted and scored by two blinded pathologists with expertise in lung pathology. The scoring system was, 0 = normal; 1 = very mild; 2 = mild; 3 = moderate; 4 = marked; 5 = severe inflammation. The total lung injury score was

expressed as the sum of the four criteria. Mean scores were derived from 12 animals.

2.6. In vivo pulmonary vascular permeability assessment

Evans blue is a dye that binds rapidly to albumin and remains restricted within blood vessels because endothelium is impermeable to albumin under normal physiological conditions (Radu and Chernoff, 2013). Pulmonary microvascular permeability was assessed by measuring the extravasation of Evans blue dye in the lungs as previously described (Yao et al., 2011). Briefly, mice were randomly divided into control group (12 mice) and LPS group (48 mice) while LPS group mice were further divided into four subgroups. For pulmonary microvascular permeability assessment, unanesthetized mice of LPS group received intragastric instillation of NS, CT-133 at 10 or 30 mg/kg and Dex at 1 mg/kg respectively. After 1 h, anesthetized mice were subjected to intratracheal instillation of NS to control group and LPS to all LPS subgroups at 10 μl/10 g of body weight. Twenty-four hours after LPS challenge, Evans blue dye (50 mg/kg) was injected into the caudal vein of all mice 1 h before euthanasia. After killing the mice, NS was gently injected into the right ventricle in order to drain the blood from pulmonary vessels. Right lungs were carefully removed, sliced and placed in formamide (3 ml/100 mg) at room temperature. After 24 h of incubation, samples were centrifuged at $500 \times g$ for 10 min (4 °C), and then the absorbance of Evans blue dye extracted in the supernatant was determined against formamide blank at 620 nm via standard curve method and expressed as microgram dye per 100 mg of wet lung weight. Additionally, albumin determination kits were used to measure the albumin concentration in BAL fluid with a spectrophotometer at 628 nm. Albumin concentrations ratio assessed from BAL fluid represent not only the effused albumin level but also the pulmonary

microvascular permeability (Xu et al., 2008).

2.7. Determination of MPO activity

The previously described procedure was slightly modified and followed for the determination of MPO activity (Lei et al., 2018). Strips of left lung tissue were accurately weight and homogenized with prepared homogenate medium (sample and homogenate medium at a ratio of 1:19) to obtain 5% homogenate. Then 5% homogenate (0.9 ml) and reaction buffer (0.1 ml) at the ratio of 9:1 were sufficiently mixed (if there is not enough homogenate, then volumes of 5% tissue homogenate and reaction buffer can be decreased accordingly at the ratio of 9:1), and incubated at 37 °C for 15 min. Afterward, MPO activity was determined via standard curves by measuring the changes in absorbance at 460 nm with a spectrophotometer.

2.8. Isolation of neutrophils and evaluation of PGD2-induced in vitro neutrophils migration

Isolation of neutrophils and the effect of CT-133 on neutrophils migration was evaluated by following the previously described procedure (Zhang et al., 2017). Briefly, neutrophils were isolated from peritoneal lavage of anesthetized mice 4 h after intraperitoneal injection of 1.5% glycogen (20 ml/kg of body weight). Migration of neutrophils was evaluated by using Boyden chamber assay kit (3 μm pore size; Billerica, MA). PGD_2 was used as a chemoattractant because activated PGD_2/CRTH2 receptors promote neutrophil migration (Ishii et al., 2012; Jandl et al., 2016). Initially, isolated neutrophils at 4×10^5 cell/ml were seeded in the upper side of well of Boyden chamber, while lower chamber contained different concentrations of PGD_2 (0.1, 1 and 10 μM), and neutrophils were allowed to migrate toward PGD_2 for 4 h at 37 °C in order to find out the suitable PGD_2 concentration. After evaluation of the suitable PGD_2 concentration, migration of neutrophils pretreated with CT-133 (1 and 10 μM) and OC459 (10 μM), another potent CRTH2 inhibitor, toward PGD_2 (1 μM) was accessed with 4 h.

2.9. Isolation of peritoneal macrophages and measurement of PGD_2 secretion from LPS-treated peritoneal macrophages

The previously described procedure was slightly modified and adopted to isolate the peritoneal macrophages from mice (Davies and Gordon, 2005). Briefly, 4% thioglycollate (20 ml/kg of body weight) was intraperitoneally injected to mice for three consecutive days. Forty-eight hours after last thioglycollate injection (on the 5th day), peritoneal macrophages were isolated from the peritoneal cavity of euthanized mice, added to12-well plates (4×10^5/well) and allowed to culture at 37 °C. Non-adherent cells are removed by gently washing three times with warm PBS. At this time, more than 90% are macrophage and allowed to the culture at 37 °C in DMEM/high glucose containing 10% FBS in the presence of penicillin (100U/ml) and streptomycin (100 μg/ml). After acclimation, serum-free DMEM/high glucose was added to 12-well plates for 10–12 h and then treated with different concentrations of LPS (0.01, 0.1, 1 and 10 μM) for next 24 h. Afterward, the supernatants of the treated peritoneal macrophages were harvested to measure the level of PGD_2 using ELISA kit according to the manufacturer's instructions.

2.10. Cell culture and cell viability assay

RAW264.7 macrophage, mouse leukemic monocyte macrophage, cell line was purchased from ATCC (Manassas, VA), and cultured in RPMI-1640 medium containing 10% fetal bovine serum supplemented with 100 μg/ml streptomycin and 100 U/ml penicillin. RAW264.7 macrophage is an excellent model for screening the anti-inflammatory drugs and evaluating the inhibitors of pathways that stimulate the production of pro-inflammatory cytokines and enzymes. The cytotoxicity of CT-133 alone as well as in the combination of LPS and PGD_2 on RAW264.7 macrophages and isolated peritoneal macrophages was assessed using a methylthiazol-tetrazolium (MTT) assay according to the manufacturer's protocol. Briefly, macrophages were plated at a concentration of 4×10^5 cells/ml in 96-well plates for 12 h and subsequently exposed to CT-133 at the dose range of 0–200 μM for 1 h at 37 °C. Next, macrophages were further exposed to LPS (100 ng/ml) and PGD_2 (10 μM) for 24 h, followed by treatment with MTT (5 mg/ml) for an additional 4 h at 37 °C. Then, the supernatant of each well was replaced with DMSO (200 μl/well) and absorbance was measured at 570 nm.

2.11. In vitro ELISA assay and real-time polymerase chain reaction (RT-PCR) analysis

For ELISA and RT-PCR, RAW264.7 macrophages were acclimated to two 12-well plates at 70–80% confluence. After that, the culture medium of 12-well plates was replaced with a serum-free RPMI-1640 medium for 10–12 h and then exposed to CT-133 (10 and 100 μM) for 1 h. One hour later, one 12-well plate was treated with LPS (100 ng/ml) and other one with PGD_2 (10 μM) for 24 h. After treatment, the supernatants of the cells with different treatments were harvested to measure the protein levels of IL-1β, TNF-α, IL-6, and KC using ELISA kits according to the manufacturer's instructions. Subsequently, Total RNA from each treated plates were extracted and reversely transcribed into cDNA with HiScript $5 \times$ Q RT SuperMix, and then subjected to RT-PCR using BioRad CFX96 Touch™ Real-Time PCR Detection System (San Diego, CA). Similarly, Total RNAs extracted from treated isolated peritoneal macrophages were subjected to analyse the mRNA levels of IL-1β, TNF-α, IL-6, and KC. The primers used for RT-PCR reaction are depicted in Table 1. The housekeeping gene, β-actin, was used as an internal control. RT-PCR reactions were triplicated and the relative expression of the target mRNA was normalized by the respective β-actin.

2.12. Western blot assays

Total protein extraction and Western blot assays were performed according to the previously described method (Xu et al., 2018). Briefly, lung tissues were homogenized in RIPA buffer (0.5M Tris-HCl, pH 7.4, 1.5M NaCl, 2.5% deoxycholic acid, 10% NP-40, 10 mM EDTA) containing proteinase and phosphatase inhibitors (Sigma-Aldrich, St. Louis, MO). RAW264.7 macrophages were seeded to two 6-well plates at 70–80% confluence. After overnight starvation with a serum-free RPMI-1640 medium, RAW264.7 macrophages were pretreated with CT-133 (0.5, 1, 10 and 100 μM) for 1 h. Soon after, one 6-well plate was treated with LPS (100 ng/ml) and other one with PGD_2 (10 μM) for 1 h. After washing three times with PBS, cells were directly lysed by RIPA buffer containing proteinase and phosphatase inhibitors for 30 min at the ice with occasional shaking. Afterward, the lysate was centrifuged at

Table 1
Primers used for RT-PCR.

Genes	Primer sequences (5′ – 3′)	Product Length (bp)
IL-6	F: TGCCTTCTTGGGACTGAT	183
	R: TTGCCATTGCACAACTCTTT	
TNF-α	F: CCAGACCCTCACACTCAGAT	187
	R: GACAAGGTACAACCCATCG	
IL-1β	F: GTTCCCATTAGACAACTGC	199
	R: GATTCTTTCCTTTGAGGC	
KC	F:CAATGAGCTGCGCTGTCAGTG R: CTTGGGGACACCTTTTAGCATC	203
β-actin	F: CACGATGGAGGGGCCGGACTCATC	214
	R: TAAAGACCTCTATGCCAACACAGT	

$12,300 \times g$ for 15 min at 4 °C and the supernatant was collected. Bradford protein assay (BCA) was performed to measure protein concentrations. Equal amounts of protein (30 μg) were resolved on 12% SDS-PAGE and transferred to 0.45 μm polyvinylidene fluoride (PVDF) membranes (Millipore, Bedford, MA). The membranes were blocked with 5% (wt/vol) non-fat dried milk for 1–2 h at room temperature to reduce nonspecific binding. The membranes were then incubated with primary antibodies specific to IκBα (1:1000), phospho-Iκ Bα (1:1000), NF-κB P65 (1:1000), phospho- NF-κB P65 (1:1000) at 4 °C overnight and secondary antibodies IRDye 680 and 800 at room temperature for 1 h, followed by washing with TBST three times. The immunoreactive signals were visualized with Odyssey Infrared Imaging System (LI-COR Biosciences Lincoln, NE). Western blot assays were triplicated and β-actin was used as an internal standard. The same procedure was performed for the lungs after homogenization.

2.13. Statistics

Numerical data were expressed as means ± S.E.M., and statistical calculations were performed using SPSS (SPSS Inc., Chicago, IL). One-way ANOVA was applied to compare the F values, if $p > 0.05$, Dunnett multiple comparisons tests were used for calculating the difference of parametric data; if $P < 0.05$, Mann-Whitney U non-parametric test was used to compare the difference. $P < 0.05$ and $P < 0.01$ were considered to be statistically significant.

3. Results

3.1. CT-133 alleviated LPS-induced lung injury

Twenty-four hours after the LPS challenge, BAL fluids were collected to analyse the effect of CT-133 on the cell infiltration via Wright–Giemsa staining method. The LPS challenge enhanced the infiltration of total cells, neutrophils and macrophages when compared with the NS challenge ($P < 0.01$). However, CT-133 at 10 and 30 mg/kg significantly and dose-dependently attenuated the LPS-induced increases in total cells, neutrophils, and macrophages but not lymphocytes in the BAL fluid when compared with the vehicle-treated control group ($P < 0.01$), and CT-133 at 30 mg/kg behaved essentially the same as Dex at 1 mg/kg (Fig. 2A). Assessment of LPS-induced hypoxemia and pulmonary oedema by measuring the SO_2 and lung wet weight coefficient, respectively, revealed a lower SO_2 and a higher lung wet weight coefficient in the LPS-treated group than in the control group ($P < 0.01$), and treatment with CT-133 at 10 and 30 mg/kg significantly elevated the SO_2 ($P < 0.01$) and notably decreased the lung wet weight coefficient ($P < 0.01$) in a dose-dependent manner (Fig. 2 B and C). CT-133 at 10 or 30 mg/kg was as potent as Dex at 1 mg/kg to enhance the SO_2 and decrease the lung wet weight coefficient, respectively, indicating that CRTH2 antagonism via CT-133 could considerably ameliorate the pulmonary inflammation, hypoxemia and pulmonary oedema induced by LPS in ALI models.

3.2. CT-133 ameliorated the LPS-induced production of pro-inflammatory cytokines and chemokines in BAL fluid

The effect of CT-133 on the production of pro-inflammatory cytokines and chemokines was determined by measuring the expression levels of IL-β, TNF-α, IL-6, and KC in collected BAL fluids by using the respective ELISA kits. LPS challenge remarkably augmented the expression of IL-β, TNF-α, IL-6, and KC in comparison with vehicle challenge ($P < 0.01$), in contrast, CT-133 at 10 and 30 mg/kg and Dex at 1 mg/kg effectively reduced the production of IL-β, TNF-α, IL-6, and KC in a dose-dependent manner ($P < 0.05$ or $P < 0.01$) (Fig. 3A–D). These data imply that antagonism of CRTH2 by CT-133 protects the LPS-induced ALI mice from further pulmonary inflammation caused by proinflammatory cytokines and neutrophil chemokine production.

3.3. CT-133 abated LPS-mediated lung histopathologic changes

The protective effect of CT-133 against LPS-induced lung histopathologic alterations was examined in H&E stained and paraffin-embedded lung sections. LPS-challenged mice showed significant histopathologic changes when compared to the control mice (Fig. 4A). By contrast, LPS-challenged mice treated with CT-133 at 10 and 30 mg/kg or Dex at 1 mg/kg showed significant abatement of these histopathologic changes, and the amelioration in histopathological changes by CT-133 showed a dose dependence (Fig. 4A). The mean pathological scores, in terms of haemorrhage and infiltration of inflammatory cells and neutrophils into peribronchiolar and perivascular tissues, were significantly increased after LPS challenge when compared with vehicle challenge ($P < 0.01$), while CT-133 at 10 ($P < 0.05$) and 30 mg/kg ($P < 0.01$) or Dex at 1 mg/kg ($P < 0.01$) considerably reduced the pathological scores, with the CT-133 response again showing a dose dependence (Fig. 4B). Therefore, blockage of the CRTH2 receptor by CT-133 noticeably reduced the severity of LPS-induced lung injuries and reversed the impairments of lung tissues.

3.4. CT-133 minimised pulmonary vascular permeability

The protective effect of CT-133 on LPS-induced pulmonary vascular permeability was measured by determining the BAL fluid albumin contents and extraversion of Evans blue dye in the lungs. The BAL fluid albumin contents were substantially increased in the LPS-treated group compared to the control group ($P < 0.01$), however, CT-133 at 10 ($P < 0.05$) and 30 mg/kg ($P < 0.01$) or Dex at 1 mg/kg ($P < 0.01$) markedly reduced the BALfluid albumin contents (Fig. 5A). The pulmonary vascular leakage and quantitative extravasation of Evans blue dye were significantly higher in the LPS-challenged group than in the control group ($P < 0.01$), administration of CT-133 at 10 ($P < 0.05$) and 30 mg/kg ($P < 0.01$) or Dex at 1 mg/kg ($P < 0.01$) significantly decreased both the LPS-induced pulmonary vascular leakage and the extravasations of Evans Blue (Fig. 5B). Thus, these results suggested that CRTH2 antagonism effectively ameliorated pulmonary vascular permeability in LPS-induced ALI mice.

3.5. CT-133 decreased LPS-induced MPO activity in the lungs

MPO is produced by activated neutrophils and is an important marker of neutrophil infiltration and lung tissue damage (Moraes et al., 2006). Increases in MPO activity reflect the increased accumulation of activated neutrophils in the lung. MPO activity was significantly higher in the lung tissues from the LPS-treated mice than from the control group ($P < 0.01$). CT-133 at 10 and 30 mg/kg (both $P < 0.01$) or Dex at 1 mg/kg ($P < 0.01$) treatment markedly attenuated the MPO activity, with CT-133 again showing a dose dependence (Fig. 6A). CRTH2 receptor blockade with CT-133 therefore inhibited the infiltration of neutrophils into the alveolar and interstitial spaces.

3.6. CT-133 attenuated the in vitro PGD$_2$-induced neutrophil migration

The direct effect of CT-133 on the migration of neutrophils was evaluated using transwell assays because the primary cause of ALI symptoms is the deleterious inflammatory mediators released by neutrophils. The characteristics of isolated neutrophils were evaluated by Wright-Giemsa staining and cell viability determinations were performed (data not shown). Activated PGD$_2$/CRTH2 receptors promote neutrophil migration and its functioning (Ishii et al., 2012; Jandl et al., 2016), therefore, we used PGD$_2$ as a chemoattractant. After 4 h of incubation, a significant neutrophil migration towards PGD$_2$ ranging from 1 to 10 μM ($P < 0.05$ or $P < 0.01$) was noticed (Fig. 6B). Pretreatment of neutrophils with CT-133 at 1 and 10 μM (both $P < 0.01$) or OC459 at 10 μM ($P < 0.01$) substantially attenuated 1 μM of PGD$_2$-induced neutrophil migration (Fig. 6C). Collectively, these data indicated that
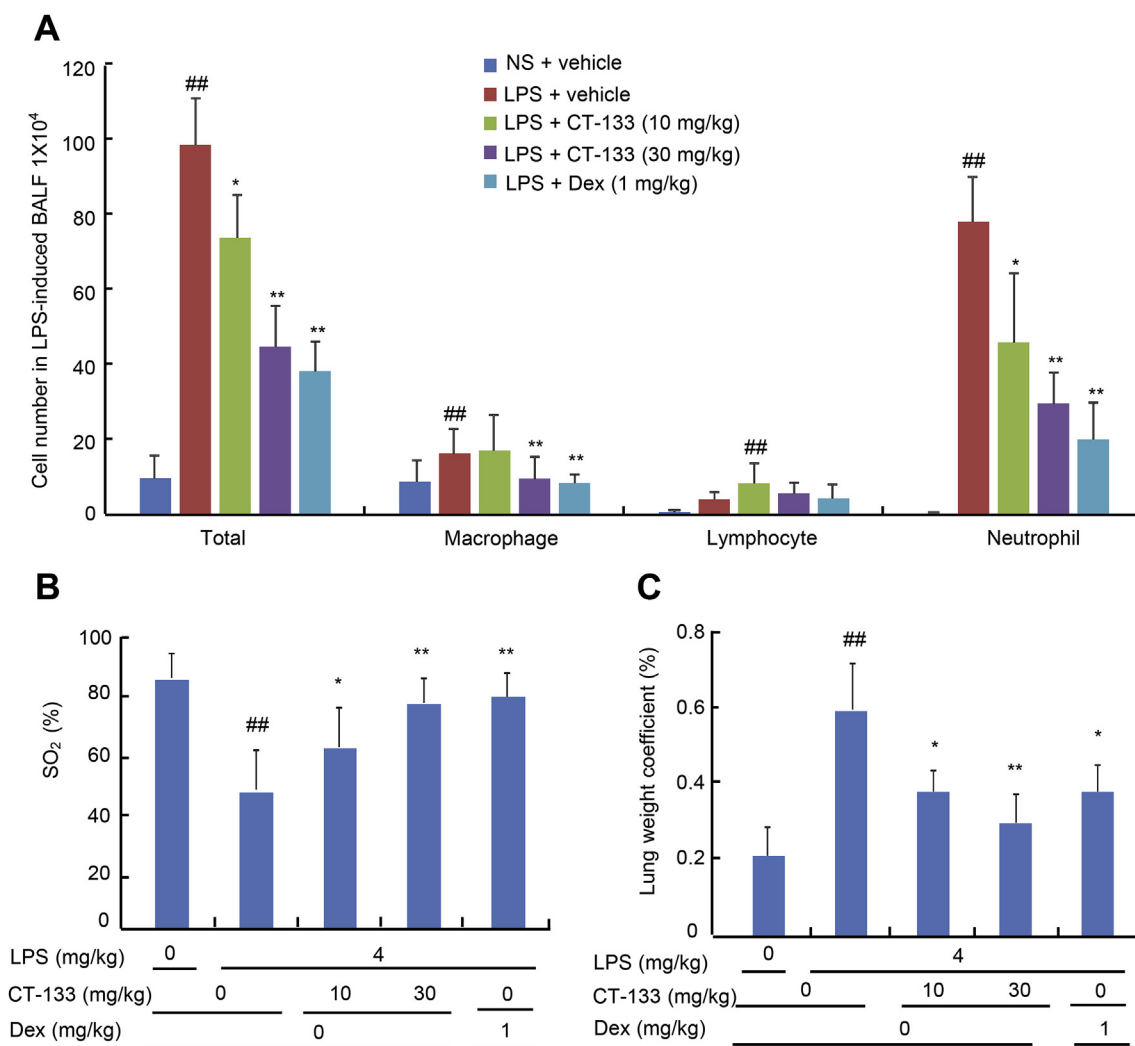
Fig. 2. Effect of CT-133 on BAL fluid inflammatory cell counting and classification, oxygen saturation (SO$_2$) and lung weight coefficient. For acute pulmonary injury, (A) CT-133 (10 and 30 mg/kg) or Dex (1 mg/kg) were intragastrically administered 1 h before and 12 h after intratracheal LPS instillation. BAL fluid was collected 24 h after the LPS challenge to calculate the total number of cells, and the numbers of neutrophils, macrophages and lymphocytes. (B) Twenty-4 h after LPS challenge, oxygen saturation (SO$_2$) was measured in all mice with a Moor VMS-OXY™ monitor. (C) Twenty-4 h after LPS challenge, lung weight coefficient was measured by dividing the individual lung weight of each mouse by its body weight. $^{##}P < 0.01$ versus NS + vehicle group; $^*P < 0.05$, $^{**}P < 0.01$ versus LPS + vehicle group. Values are expressed as mean ± S.E.M., n = 12 for each group.

CRTH2 antagonists significantly attenuated the neutrophil migration toward PGD$_2$.

3.7. LPS promoted PGD$_2$ secretion from isolated peritoneal macrophages

Isolated peritoneal macrophages were treated with different concentrations of LPS to evaluate the amounts of extracellularly secreted PGD$_2$ protein using a PGD$_2$ ELISA kit. LPS ranging from 0.01 to 10 μM (all $P < 0.01$) treatment significantly promoted the secretion of PGD$_2$ when compared to the vehicle treatment (Fig. 6D).

3.8. CT-133 reduced LPS- and PGD$_2$-induced secretion of pro-inflammatory cytokines and chemokines from RAW264.7 macrophages and isolated peritoneal macrophages

Activation of PGD$_2$/CRTH2 receptors on macrophages strikingly worsens the disease condition by over-expression of pro-inflammatory cytokines that serve as key factors in the pathogenesis of ALI (Jandl et al., 2016). Therefore, the effect of CT-133 treatment on either LPS- or PGD$_2$-induced production of pro-inflammatory factors was also examined in macrophages. The MTT assay indicated that supplying LPS at

100 ng/ml plus CT-133 at dosages up to100 μM or PGD$_2$ at 10 μM plus CT-133 at dosages up to100 μM were not toxic to RAW264.7 macrophages or isolated peritoneal macrophages (data not shown). The effects of CT-133 on the expression of pro-inflammatory cytokines and a chemokines were measured by ELISA. CT-133 at 10 and 100 μM dose-dependently inhibited the protein expression of IL-1β, TNF-α, IL-6, and KC (all $P < 0.05$ or $P < 0.01$) in response to LPS (Fig. 7A–D) or PGD$_2$ (Fig. 7E–H) stimulation. Quantitative RT-PCR demonstrated that CT-133 at 10 and 100 μM dose-dependently reduced the mRNA expression of IL-1β, TNF-α, IL-6, and KC (all $P < 0.05$ or $P < 0.01$) in either LPS- or PGD$_2$-stimulated RAW264.7 macrophages (Fig. 8A–H) and in isolated peritoneal macrophages (Fig. 9A–H). Thus, these *in vitro* results were in agreement with the *in vivo* results shown in Fig. 4 and implied that CRTH2 antagonism with CT-133 effectively ameliorated the production of pro-inflammatory cytokines and chemokines from either LPS- or PGD$_2$-activated RAW264.7 macrophages and isolated peritoneal macrophages as well.

3.9. CT-133 inhibited P65 activation in vitro and in vivo

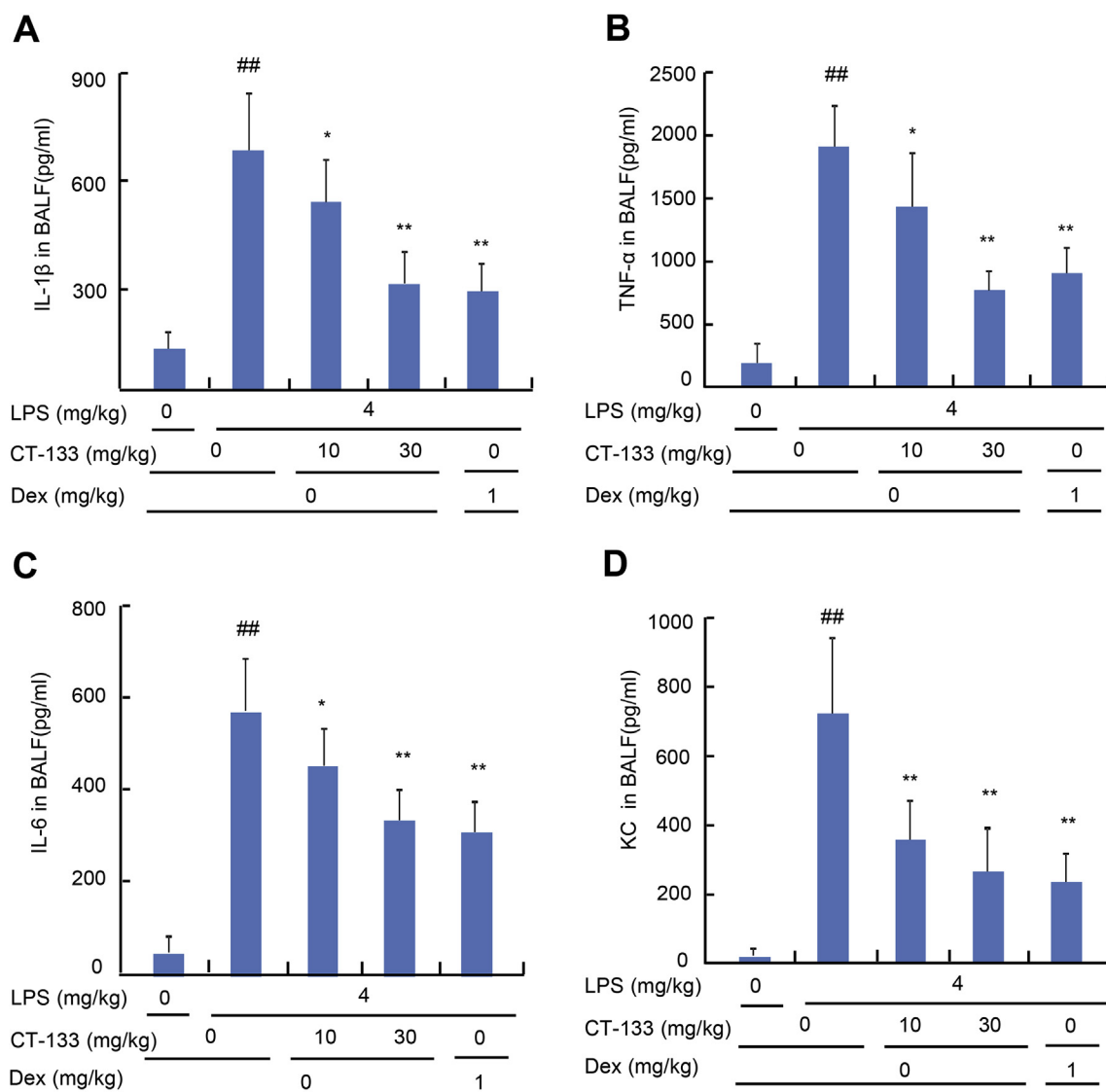The underlying mechanism by which CT-133 significantly inhibits

Fig. 3. Effect of CT-133 on pro-inflammatory cytokines (TNF-α, IL-β, IL-6) and a chemokine (KC) production in BAL fluids of LPS-induced ALI mice. BAL fluid was collected and analysed for TNF-α (A), IL-β (B), IL-6 (C) and KC (D) levels using their respective ELISA kits. $^{##}P < 0.01$ versus vehicle + vehicle group; $^{*}P < 0.05$, $^{**}P < 0.01$ versus LPS + vehicle group. Values are expressed as mean ± S.E.M., n = 12 for each group.

the LPS-induced ALI was explored by Western blot assays. This investigation focused on the effects of CT-133 on LPS-induced NF-κB pathway activation, because NF-κB is required for the activation of pro-inflammatory mediators, infiltration of neutrophils and increases in pulmonary vascular permeability (Bhatia and Moochhala, 2004; Everhart et al., 2006; Matthay et al., 2012; Yang et al., 2012). Treatment of RAW264.7 macrophages and lung tissues with LPS robustly induced the phosphorylation and degradation of IκBα, thereby increasing or decreasing the phosphorylated P65 or P65 levels, respectively, when compared with the treatment with vehicle (Fig. 10A and B). Treatment with CT-133 at 0.5, 1.0, 10, and 100 μM in RAW264.7 macrophages or at 10, and 30 mg/kg in ALI mice dose-dependently reduced the LPS-induced not only IκBα but also P65 activation and robustly reversed LPS-induced IκBα as well as P65 degradation (Fig. 10A and B). Thus, the CRTH2 receptor antagonist CT-133 protected the mice from LPS-induced ALI by most probably suppressing the NF-κB signalling.

4. Discussion

The experimental outcomes presented here are the first to reveal the

significant effect of a CRTH2 antagonist on LPS-induced lung injury. CRTH2 antagonism with CT-133 strikingly reduced many of the LPS-induced cardinal features in the mouse ALI model, including neutrophil and macrophage accumulation and pro-inflammatory cytokines and albumin production in BAL fluid, hypoxemia, lung weight coefficient increases, Evans blue exudation into the lungs, lung MPO activity and lung histopathological changes. CT-133 treatment also significantly minimised the *in vitro* PGD$_2$-induced neutrophil migration and LPS/PGD$_2$-stimulated overexpression of pro-inflammatory cytokines and a chemokine in RAW264.7 macrophages. CT-133 treatment also markedly inhibited the LPS-induced activation of NF-κB at both the *in vitro* and *in vivo* levels.

Excessive infiltration and accumulation of inflammatory cells, particularly neutrophils, in both alveolar and interstitial spaces is one of the pivotal pathological hallmarks of lung injury (Li et al., 2016; Zhou et al., 2011). A rapid and appropriate neutrophil influx is crucial for clearance of alveolar pathogens and debris; however, neutrophilia may contribute to extensive lung inflammation and substantially increased alveolar-capillary membrane permeability due to the release of several toxic mediators from the neutrophils (Bhattacharya and Matthay, 2013; Chignard and Balloy, 2000). Notably, the finding of increased numbers
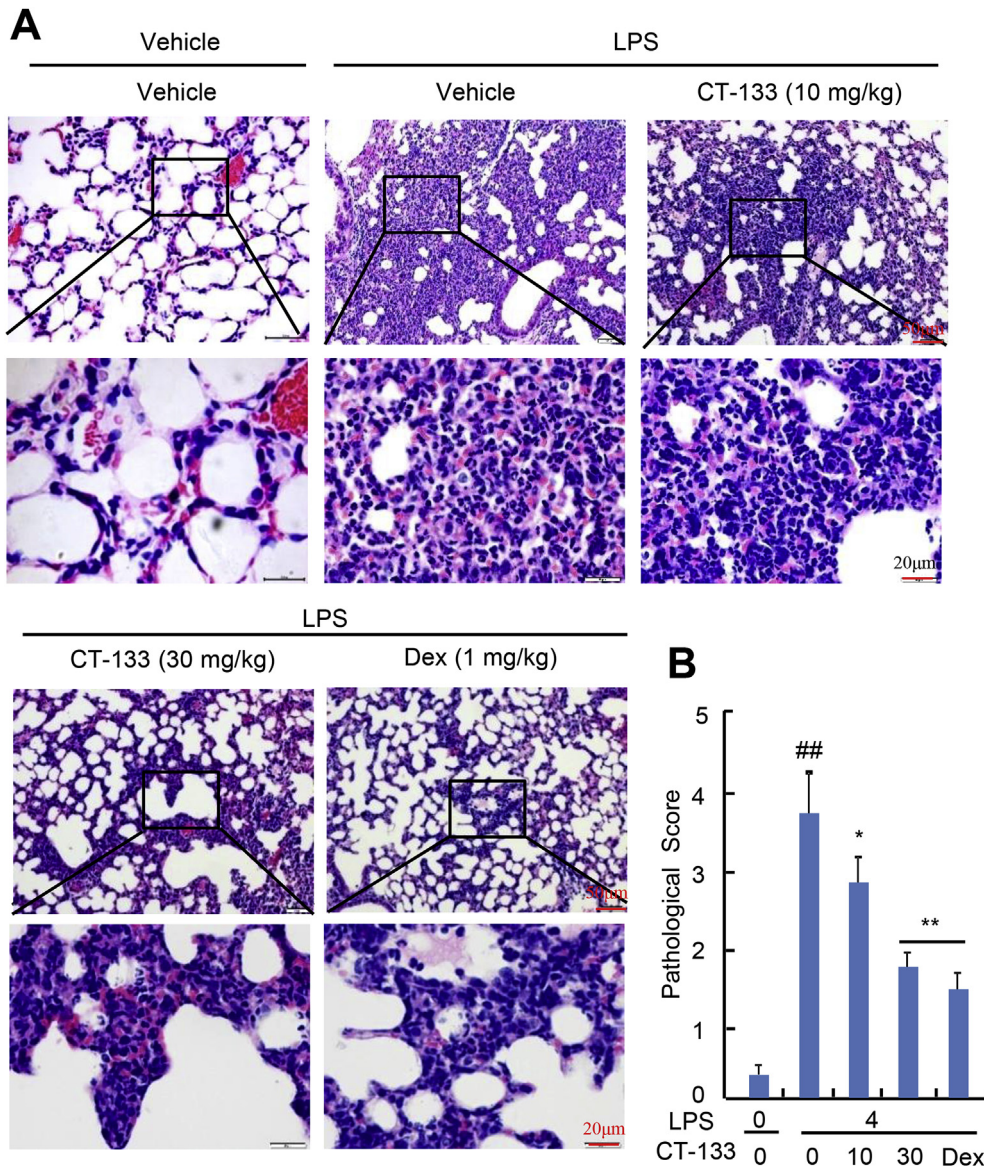
A

B

Fig. 4. Effect of CT-133 on histopathological changes in the lungs of LPS-induced ALI mice. Paraffin-embedded lung sections from each experimental group were stained with hematoxylin-eosin (H&E) for histopathological evaluation. (A) Representative images of lung tissues stained with H&E show oedema and in-filtration of neutrophils and inflammatory cells. (B) Quantitative analysis of lung injury scored by two blinded pathologists with expertise in lung pathology. $^{##}P < 0.01$ versus vehicle + vehicle group; $*P < 0.05$, $**P < 0.01$ versus LPS + vehicle group. Values are expressed as mean $\pm$ S.E.M., n = 12 for each group.
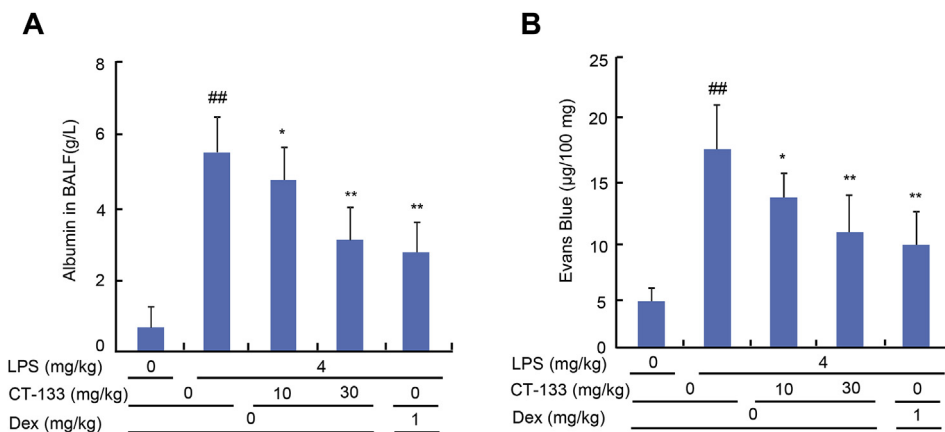
A

B

Fig. 5. Effect of CT-133 on LPS-induced pulmonary vascular permeability. Twenty-four hours after LPS challenge, (A) albumin concentration in BAL fluid was measured using albumin determination kits. (B) Evans blue dye (50 mg/kg) was injected into the caudal vein of all mice 1 h before euthanasia. Pulmonary vascular permeability was assessed by determining the accumulation of Evans blue dye in the lung tissue. $^{##}P < 0.01$ versus vehicle + vehicle group; $*P < 0.05$, $**P < 0.01$ versus LPS + vehicle group. Values are expressed as mean $\pm$ S.E.M., n = 12 for each group. (For interpretation of the references to colour in this figure legend, the reader is referred to the Web version of this article.)
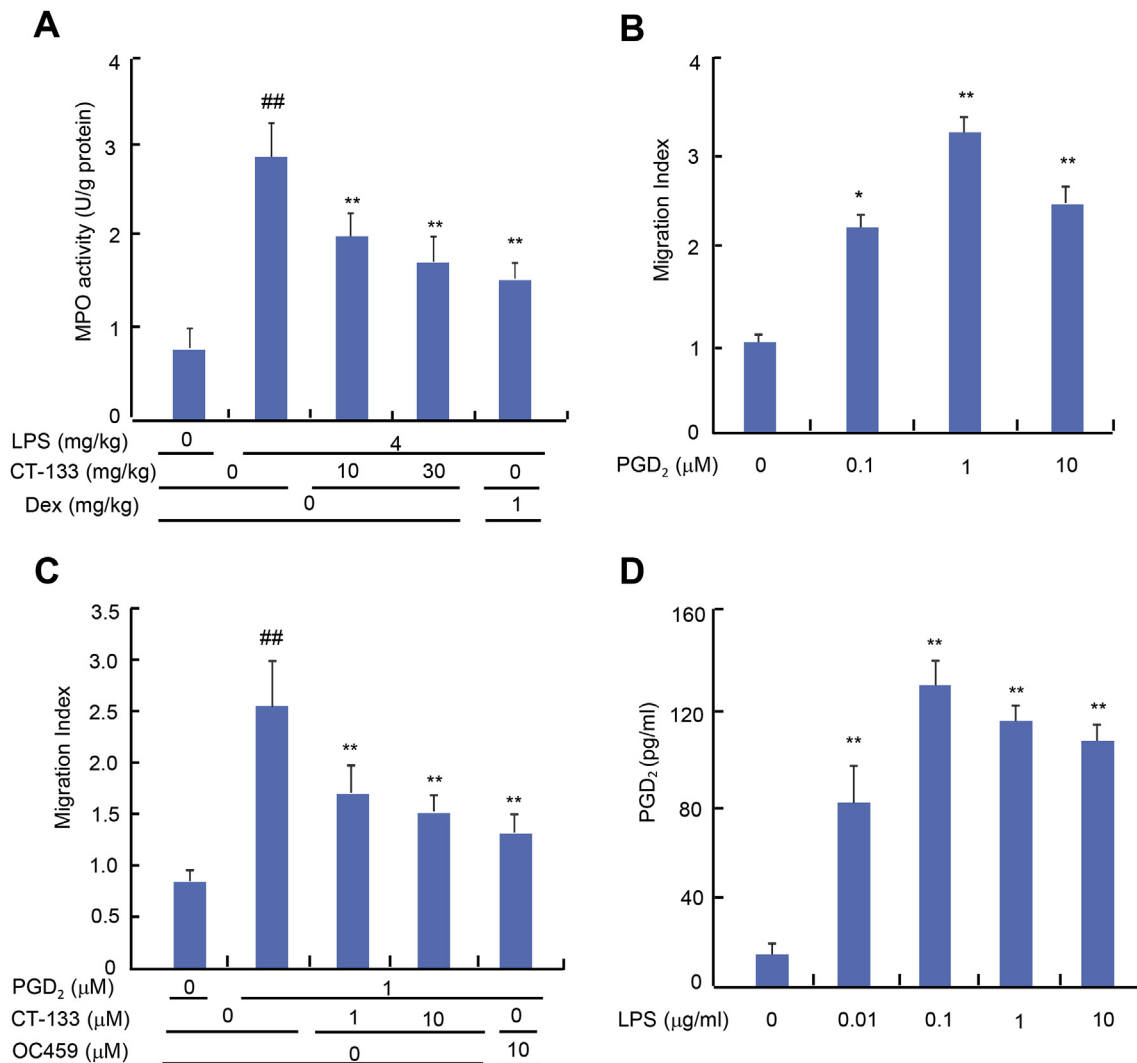
Fig. 6. Effect of CT-133 on lung MPO activity and *in vitro* PGD$_2$-induced neutrophil migration, and assessment of LPS-induced secretion of PGD$_2$ from primary macrophages. (A) MPO activity from lung homogenates was measured using MPO kits. $^{##}P < 0.01$ versus vehicle + vehicle group; $^{**}P < 0.01$ versus LPS + vehicle group. Values are expressed as mean ± S.E.M., n = 12 for each group. (B and C) PGD$_2$-induced neutrophil migration was evaluated using Boyden chamber assay kits (3 μm pore size) in the presence or absence of CT-133. $^{##}P < 0.01$ versus vehicle + vehicle group; $^{*}P < 0.05$, $^{**}P < 0.01$ versus vehicle group or PGD2 + vehicle group. Values are expressed as mean ± S.E.M., n = 3 for each group. (D) Supernatants from isolated primary macrophages pretreated with different concentrations of LPS (0.01, 0.1, 1 and 10 μM) for 24 h, were harvested to measure the protein levels of PGD$_2$ using a PGD$_2$ ELISA kit. $^{##}P < 0.01$ versus vehicle group. Values are expressed as mean ± S.E.M., n = 3 for each group.

of neutrophils in BAL fluid is closely related to the severity of lung injury (Abraham, 2003; Grommes and Soehnlein, 2011), while the severity of LPS-induced lung injury has been reduced by neutrophil depletion in mice (Chignard and Balloy, 2000; Li et al., 2016).

In LPS-induced murine models, PGD$_2$ is a critical mediator of macrophage migration (Tajima et al., 2008), and activated PGD$_2$/CRTH2 receptors on macrophages orchestrate neutrophil recruitment into the lung, augmenting the disease severity (Jandl et al., 2016). CRTH2 acts as a critical regulator of neutrophil migration (Ishii et al., 2012), because CRTH2 agonists trigger neutrophil migration (Shichijo et al., 2003), while selective CRTH2 antagonists inhibit neutrophil trafficking into the lung (Stebbins et al., 2010). Similarly, genetic ablation of CRTH2 suppresses neutrophil migration in sepsis models (Ishii et al., 2012) and increases the survival rate in ALI models (Suzuki et al., 2016). In the present study, we find that intratracheal instillation of LPS strikingly increases inflammatory cell counts, neutrophil infiltration and MPO activity in the lungs, whereas CT-133 treatment markedly ameliorates the LPS-induced increases in inflammatory cell and neutrophil numbers, reduced the MPO activity and lessened the lung

hypoxemia. These outcomes suggest that the protective effects of CT-133 might be due to an inhibition of neutrophil migration and a reduction in pulmonary vascular permeability, via a CRTH2 receptor blockade. Our further investigation confirms that CT-133 blocks PGD$_2$-induced neutrophil migration *in vitro*, and minimises the LPS-induced accumulation of albumin in BAL fluid, Evans blue accumulation in lungs and pulmonary oedema. Lung histological examinations and lung injury scores also show that CT-133 attenuates the LPS-induced alveolar wall damage, neutrophil infiltration and lung tissue injury.

Apart from neutrophil-mediated inflammation, the production of pro-inflammatory cytokines and chemokines from PGD$_2$/CRTH2 activated macrophages could further aggravate LPS-induced lung injury (Eguchi et al., 2011; Jandl et al., 2016). Interestingly, genetic ablation of CRTH2 diminishes the TNF-α production in sepsis, a common cause of ALI (Ishii et al., 2012). However, the macrophage-derived IL-1β and TNF-α, as early response cytokines following LPS-induced lung injury, elicit an inflammatory cascade through direct damage to the vascular endothelial and alveolar epithelial cells. This results in the secretion of another pro-inflammatory cytokine, such as IL-6 (Mukhopadhyay et al.,
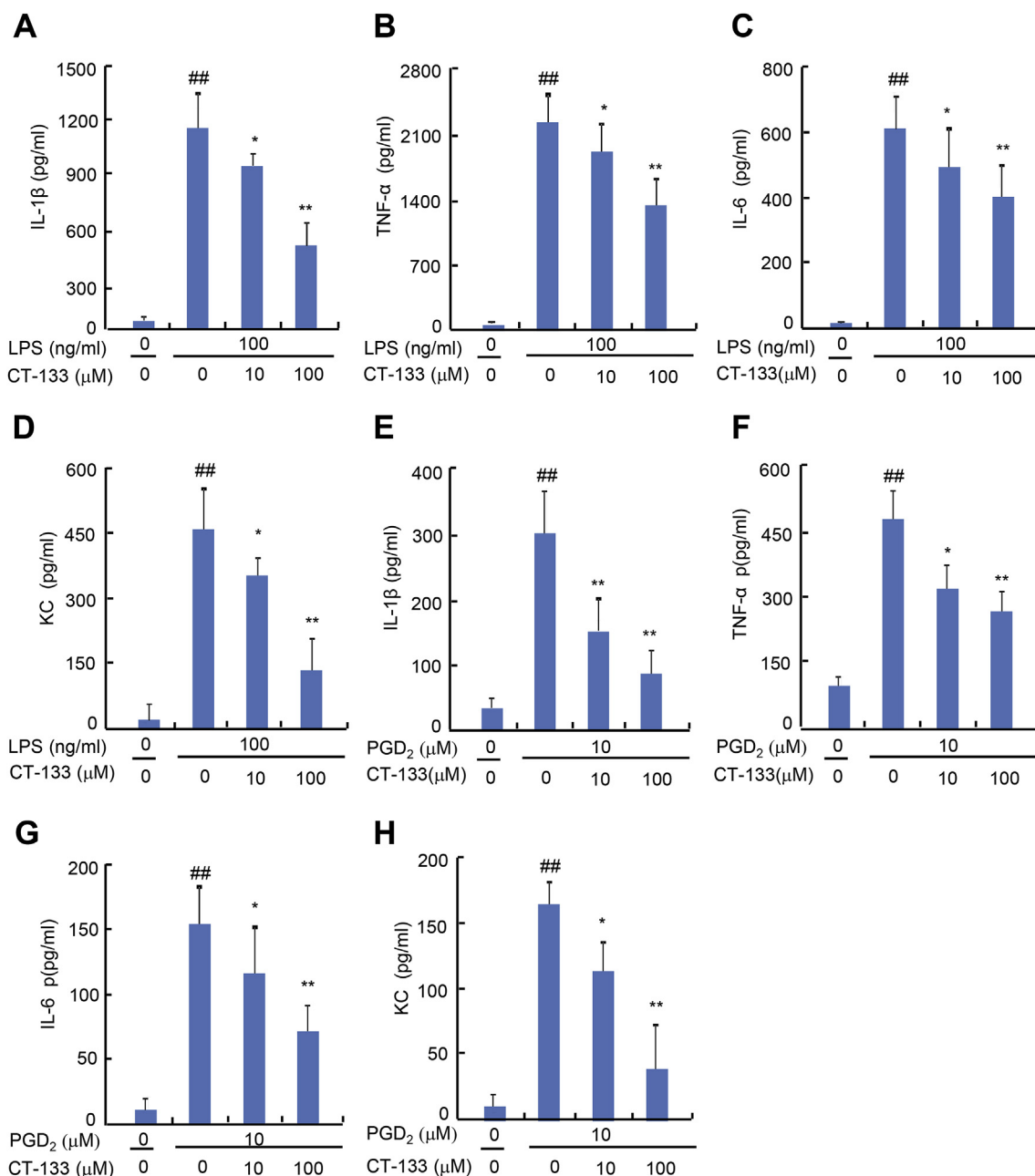
Fig. 7. Effect of CT-133 on pro-inflammatory cytokines (TNF-α, IL-β, IL-6) and a chemokine (KC) secreted from LPS- or PGD$_2$-stimulated RAW264.7 macrophages. RAW264.7 macrophages were pretreated with CT-133 for 1 h and further treated with CT-133 and LPS/PGD$_2$ for 24 h, and then the culture medium was harvested to measure the levels of secreted IL-β (A and E), TNF-α (B and F), IL-6 (C and G) and KC (D and H) using respective ELISA kits. $^{##}P < 0.01$ versus vehicle + vehicle group; $*P < 0.05$, $**P < 0.01$ versus LPS/PGD2 + vehicle group. Values are expressed as mean ± S.E.M., n = 3 for each group.

2006) and neutrophil chemokines, such as IL-8 (Kim et al., 2010), thereby further intensifying the inflammation process. Notably, pro-inflammatory cytokines including IL-1β, TNF-α, and IL-6 (Strieter and Kunkel, 1994) and a chemokine IL-8 (Hammond et al., 1995; Singer and Sansonetti, 2004) trigger an intense migration of neutrophils across the endothelial barrier. Elevated levels of pro-inflammatory cytokines and chemokines have been identified in BAL fluid of patients with ALI/ARDS (Goodman et al., 1996), while attenuation of pro-inflammatory cytokines and chemokines levels in LPS-induced animal models leads to the reduced lung injury (Li et al., 2016). Similarly, in our study, LPS exposure increases the expression of IL-1β, TNF-α, IL-6 and KC (the mouse homologue of IL-8) in the BAL fluid of the murine ALI model mice, when compared with control mice. However, CT-133 treatment markedly suppresses this overexpression by blocking CRTH2. Likewise,

the ELISA and RT-PCR results reveal that LPS and PGD$_2$ treatments of RAW264.7 macrophages cause an overproduction of IL-1β, TNF-α, IL-6 and KC that closely reflects the pathogenesis of ALI (Hou et al., 2018). CT-133 pretreatment noticeably inhibits this LPS- and PGD$_2$-induced overexpression. We also find that macrophage number is much lower in the CT-133-treated (30 mg/kg) group than in the LPS treated group, suggesting that CRTH2 antagonism alters the macrophage influx and alleviates the damage due to the pro-inflammatory mediators in the LPS-induced mouse ALI model.

NF-κB plays a pivotal role in the transcriptional regulation of various inflammation-related genes. Elevated NF-kB levels have been reported in LPS-induced ALI murine models (Xu et al., 2011; Yu et al., 2013), and pharmacological inhibition of the NF-kB pathway significantly decreases airway inflammation by inhibiting the MPO
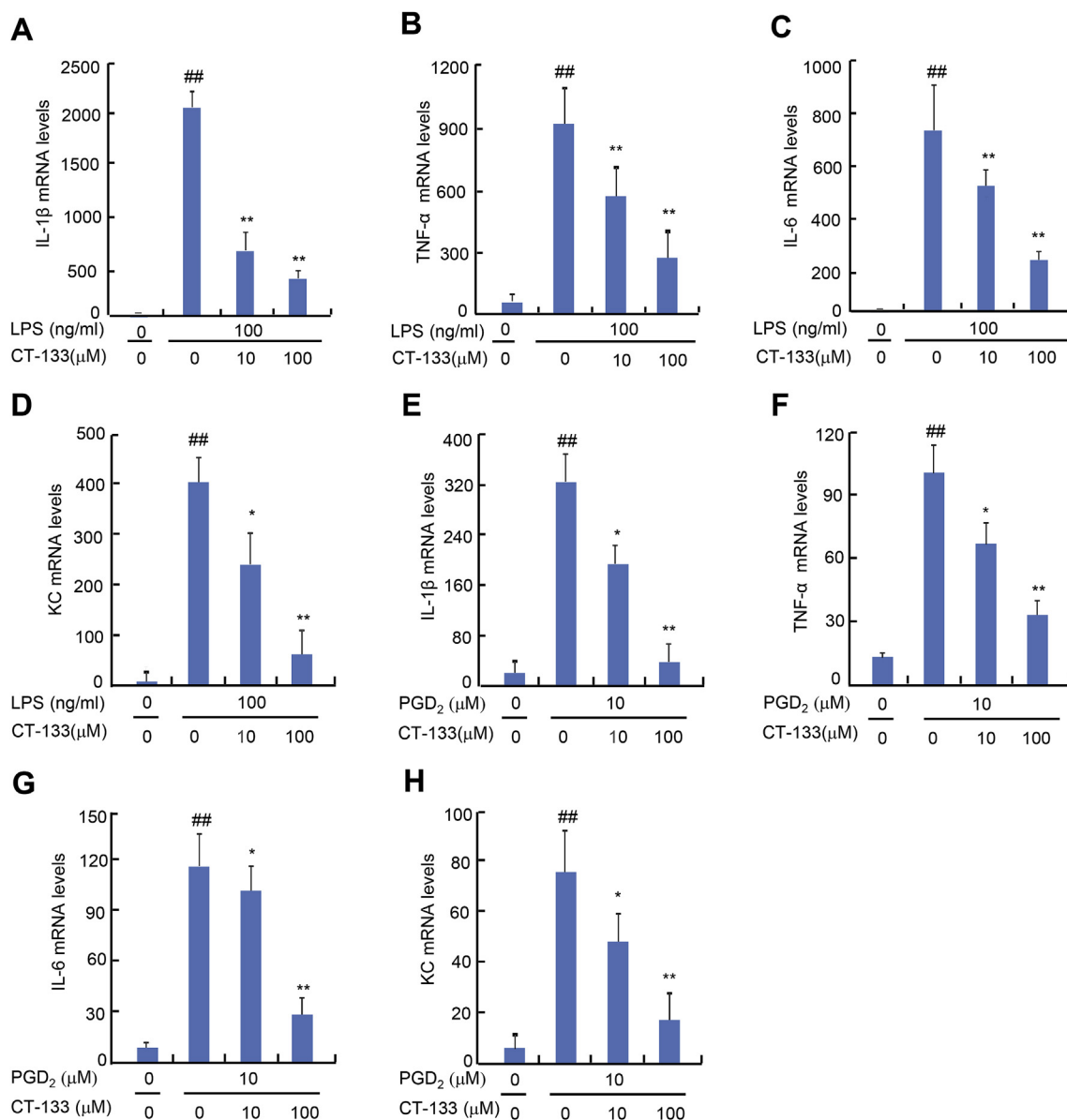
Fig. 8. Effect of CT-133 on mRNA expression of pro-inflammatory cytokines (TNF-α, IL-β, IL-6) and a chemokine (KC) in LPS- or PGD₂-stimulated RAW264.7 macrophages. RAW264.7 macrophages were pretreated with CT-133 for 1 h and further treated with CT-133 and LPS/PGD₂ for 24 h, and then RNA was extracted and for analysis of the expression of IL-β (A and E), TNF-α (B and F), IL-6 (C and G) and KC (D and H) using RT-PCR. $^{\#\#}P < 0.01$ versus control group; $^{*}P < 0.05$, $^{**}P < 0.01$ versus model groups. $^{\#\#}P < 0.01$ versus vehicle + vehicle group; $^{*}P < 0.05$, $^{**}P < 0.01$ versus LPS/PGD2 + vehicle group. Values are expressed as mean ± S.E.M., n = 3 for each group.

section, pulmonary vascular permeability and pro-inflammatory mediator production (Feng et al., 2015; Nathens et al., 1997). Inhibition of NF-κB activation also suppresses the pathological changes in murine ALI models (Oishi et al., 2012). Accumulated evidence has revealed that NF-κB activation is accompanied by phosphorylation and degradation of IκBα, which ultimately promotes P65 phosphorylation and translocation into the nucleus, where it drives expression of specific target genes (Scott et al., 1993). In our study, we find that an LPS challenge significantly increased IκBα and P65 phosphorylation in the lung tissues and RAW264.7 macrophages, whereas CT-133 treatment dose-dependently and markedly inhibits the activation of NF-κB signalling. Taken together, these findings indicate that the inhibition of the NF-kB pathway plays a role in the protection of CT-133 against LPS-induced ALI.

5. Conclusion

Taken together, this study confirms that CRTH2 antagonism with CT-133 has a potent protective effect against LPS-induced ALI. This effect arises through attenuation of alveolar neutrophil and macrophage infiltration, reductions in pulmonary vascular permeability, and amelioration of the production of pro-inflammatory cytokines and chemokine production. The underlying mechanism is possibly related to an inhibition of the NF-κB signalling pathway. Therefore, CRTH2 appears to be a novel and promising candidate target for the future management of ALI.
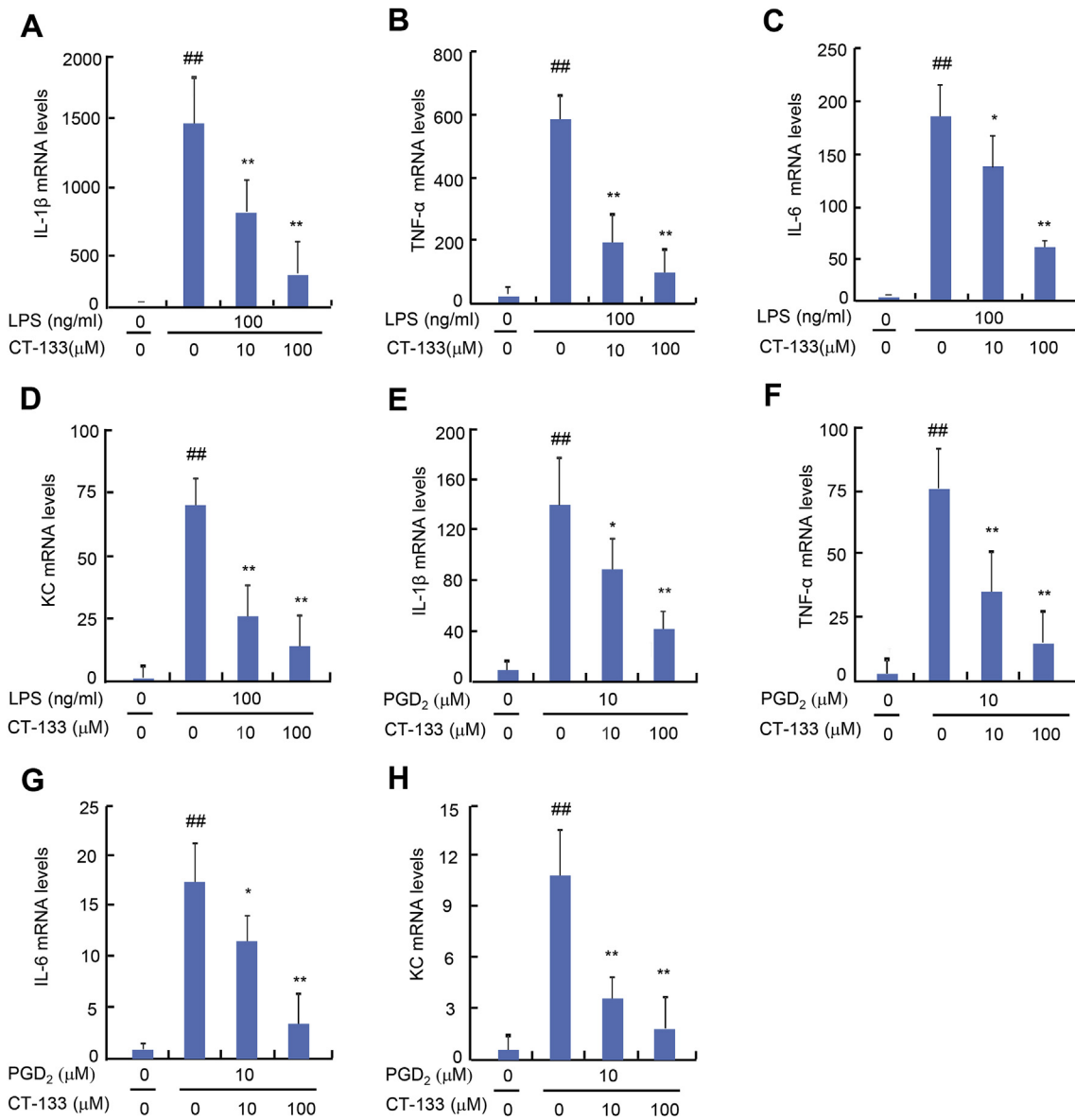
Fig. 9. Effect of CT-133 on mRNA expression of pro-inflammatory cytokines (TNF-α, IL-β, IL-6) and a chemokine (KC) in LPS- and PGD₂-stimulated primary macrophages. Primary macrophages were pretreated with CT-133 for 1 h and further treated with CT-133 and LPS/PGD₂ for 24 h, and then total RNA was extracted for analysis of expression of IL-β (A and E), TNF-α (B and F), IL-6 (C and G) and KC (D and H) using RT-PCR. $^{\#\#}P < 0.01$ versus vehicle + vehicle group; $^{*}P < 0.05$, $^{**}P < 0.01$ versus LPS/PGD2 + vehicle group. Values are expressed as mean ± S.E.M., n = 3 for each group.
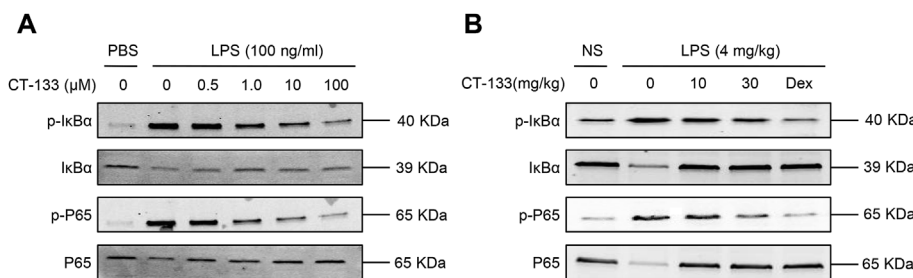

Fig. 10. Effect of CT-133 on the activation of NF-κB signalling pathway in response to LPS-stimulation in RAW 264.7 macrophages or lungs. (A) RAW264.7 macrophages were pretreated with CT-133 (0.5, 1, 10 and 100 μM) for 1 h before LPS (100 ng/ml) treatment for 1 h. (B) Preserved lung tissues were homogenized in RIPA buffer to extract the total protein. Total proteins were subjected to Western blot analysis with the indicated antibodies. β-actin was used as an internal control. All experiments were repeated at least three times.

Appendix A. Supplementary data

Supplementary data to this article can be found online at https://

Conflicts of interest

References

Abraham, E., 2003. Neutrophils and acute lung injury. Crit. Care Med. 31, S195–S199.

Bellani, G., Laffey, J.G., Pham, T., Fan, E., Brochard, L., Esteban, A., Gattinoni, L., Van Haren, F., Larsson, A., McAuley, D.F., 2016. Epidemiology, patterns of care, and mortality for patients with acute respiratory distress syndrome in intensive care units in 50 countries. J. Am. Med. Assoc. 315, 788–800.

Bhatia, M., Moochhala, S., 2004. Role of inflammatory mediators in the pathophysiology of acute respiratory distress syndrome. J. Pathol. 202, 145–156.

Bhattacharya, J., Matthay, M.A., 2013. Regulation and repair of the alveolar-capillary barrier in acute lung injury. Annu. Rev. Physiol. 75, 593–615.

Chignard, M., Balloy, V., 2000. Neutrophil recruitment and increased permeability during acute lung injury induced by lipopolysaccharide. Am. J. Physiol. Lung Cell Mol. Physiol. 279, L1083–L1090.

Davies, J.Q., Gordon, S., 2005. Isolation and Culture of Murine Macrophages, Basic Cell Culture Protocols. Springer, pp. 91–103.

Dhaliwal, K., Scholefield, E., Ferenbach, D., Gibbons, M., Duffin, R., Dorward, D.A., Morris, A.C., Humphries, D., MacKinnon, A., Wilkinson, T.S., 2012. Monocytes control second-phase neutrophil emigration in established lipopolysaccharide-induced murine lung injury. Am. J. Respir. Crit. Care Med. 186, 514–524.

Eguchi, M., Kariya, S., Okano, M., Higaki, T., Makihara, S., Fujiwara, T., Nagata, K., Hirai, H., Narumiya, S., Nakamura, M., 2011. Lipopolysaccharide induces proinflammatory cytokines and chemokines in experimental otitis media through the prostaglandin D2 receptor (DP)-dependent pathway. Clin. Exp. Immunol. 163, 260–269.

Everhart, M.B., Han, W., Sherrill, T.P., Arutiunov, M., Polosukhin, V.V., Burke, J.R., Sadikot, R.T., Christman, J.W., Yull, F.E., Blackwell, T.S., 2006. Duration and intensity of NF-κB activity determine the severity of endotoxin-induced acute lung injury. J. Immunol. 176, 4995–5005.

Feng, G., Sun, B., Li, T.z., 2015. Daidzein attenuates lipopolysaccharide-induced acute lung injury via toll-like receptor 4/NF-kappaB pathway. Int. Immunopharmacol. 26, 392–400.

Gonem, S., Berair, R., Singapuri, A., Hartley, R., Laurencin, M.F., Bacher, G., Holzhauer, B., Bourne, M., Mistry, V., Pavord, I.D., 2016. Fevipiprant, a prostaglandin D_2 receptor$_2$ antagonist, in patients with persistent eosinophilic asthma: a single-centre, randomised, double-blind, parallel-group, placebo-controlled trial. Lancet Resp. Med. 4, 699–707.

Goodman, R.B., Strieter, R.M., Martin, D.P., Steinberg, K.P., Milberg, J.A., Maunder, R.J., Kunkel, S.L., Walz, A., Hudson, L.D., Martin, T.R., 1996. Inflammatory cytokines in patients with persistence of the acute respiratory distress syndrome. Am. J. Respir. Crit. Care Med. 154, 602–611.

Grommes, J., Soehnlein, O., 2011. Contribution of neutrophils to acute lung injury. Mol. Med. 17, 293.

Guo, D., 2015. The *in vivo* profile of CT133, a potent, well tolerated, and selective CRTH2 antagonist for the treatment of allergic asthma and rhinitis. J. Allergy Clin. Immunol. 135, AB3.

Hammond, M., Lapointe, G.R., Feucht, P.H., Hilt, S., Gallegos, C.A., Gordon, C.A., Giedlin, M.A., Mullenbach, G., Tekamp-Olson, P., 1995. IL-8 induces neutrophil chemotaxis predominantly via type I IL-8 receptors. J. Immunol. 155, 1428–1433.

Herridge, M.S., Moss, M., Hough, C.L., Hopkins, R.O., Rice, T.W., Bienvenu, O.J., Azoulay, E., 2016. Recovery and outcomes after the acute respiratory distress syndrome (ARDS) in patients and their family caregivers. Intensive Care Med. 42, 725–738.

Hou, W., Hu, S., Su, Z., Wang, Q., Meng, G., Guo, T., Zhang, J., Gao, P., 2018. Myricetin attenuates LPS-induced inflammation in RAW 264.7 macrophages and mouse models. Future Med. Chem. 10, 2253–2264.

Hussain, M., Xu, C., Ahmad, M., Majeed, A., Lu, M., Wu, X., Tang, L., Wu, X., 2018. Acute respiratory distress syndrome: bench-to-bedside approaches to improve drug development. Clin. Pharmacol. Ther. 104, 484–494.

Hussain, M., Xu, C., Yao, M., Zhang, Q., Wu, J., Wu, X., Lu, M., Tang, L., Wu, F., Wu, X., 2019. CRTH2 antagonist, CT-133, effectively alleviates cigarette smoke-induced acute lung injury. Life Sci. 216, 156–167.

Ishii, M., Asano, K., Namkoong, H., Tasaka, S., Mizoguchi, K., Asami, T., Kamata, H., Kimizuka, Y., Fujiwara, H., Funatsu, Y., 2012. CRTH2 is a critical regulator of neutrophil migration and resistance to polymicrobial sepsis. J. Immunol. 188, 5655–5664.

Jandl, K., Stacher, E., Bálint, Z., Sturm, E.M., Maric, J., Peinhaupt, M., Luschnig, P., Aringer, I., Fauland, A., Konya, V., 2016. Activated prostaglandin D_2 receptors on macrophages enhance neutrophil recruitment into the lung. J. Allergy Clin. Immunol. 137, 833–843.

Karin, M., 1999. The beginning of the end: IκB kinase (IKK) and NF-κB activation. J. Biol. Chem. 274, 27339–27342.

Karin, M., Ben-Neriah, Y., 2000. Phosphorylation meets ubiquitination: the control of NF-κB activity. Annu. Rev. Immunol. 18, 621–663.

Kim, G.Y., Lee, J.W., Ryu, H.-C., Wei, J.D., Seong, C.M., Kim, J.H., 2010. Proinflammatory cytokine IL-1β stimulates IL-8 synthesis in mast cells via a leukotriene B4 receptor2-linked pathway, contributing to angiogenesis. J. Immunol. 184, 3946–3954.

Krug, N., Gupta, A., Badorrek, P., Koenen, R., Mueller, M., Pivovarova, A., Hilbert, J., Wetzel, K., Hohlfeld, J.M., Wood, C., 2014. Efficacy of the oral chemoattractant receptor homologous molecule on TH2 cells antagonist BI 671800 in patients with seasonal allergic rhinitis. J. Allergy Clin. Immunol. 133, 414–419.

Lei, J., Wei, Y., Song, P., Li, Y., Zhang, T., Feng, Q., Xu, G., 2018. Cordycepin inhibits LPS-induced acute lung injury by inhibiting inflammation and oxidative stress. Eur. J. Pharmacol. 818, 110–114.

Li, Y., Huang, J., Foley, N.M., Xu, Y., Li, Y.P., Pan, J., Redmond, H.P., Wang, J.H., Wang, J., 2016. B7H3 ameliorates LPS-induced acute lung injury via attenuation of neutrophil migration and infiltration. Sci. Rep. 6, 31284.

Matthay, M.A., Ware, L.B., Zimmerman, G.A., 2012. The acute respiratory distress syndrome. J. Clin. Investig. 122, 2731–2740.

Matute-Bello, G., Downey, G., Moore, B.B., Groshong, S.D., Matthay, M.A., Slutsky, A.S., Kuebler, W.M., 2011. An official American Thoracic Society workshop report: features and measurements of experimental acute lung injury in animals. Am. J. Respir. Cell Mol. Biol. 44, 725–738.

Moraes, T.J., Zurawska, J.H., Downey, G.P., 2006. Neutrophil granule contents in the pathogenesis of lung injury. Curr. Opin. Hematol. 13, 21–27.

Mrozek, J.D., Smith, K.M., Bing, D.R., Meyers, P.A., Simonton, S.C., Connett, J.E., Mammel, M.C., 1997. Exogenous surfactant and partial liquid ventilation: physiologic and pathologic effects. Am. J. Respir. Crit. Care Med. 156, 1058–1065.

Mukhopadhyay, S., Hoidal, J.R., Mukherjee, T.K., 2006. Role of TNFα in pulmonary pathophysiology. Respir. Res. 7, 125.

Nathens, A.B., Bitar, R., Davreux, C., Bujard, M., Marshall, J.C., Dackiw, A.P., Watson, R.W., Rotstein, O.D., 1997. Pyrrolidine dithiocarbamate attenuates endotoxin-induced acute lung injury. Am. J. Respir. Cell Mol. Biol. 17, 608–616.

Oishi, H., Takano, K.I., Tomita, K., Takebe, M., Yokoo, H., Yamazaki, M., Hattori, Y., 2012. Olprinone and colforsin daropate alleviate septic lung inflammation and apoptosis through CREB-independent activation of the Akt pathway. Am. J. Physiol. Lung. Cell Mol. 303, L130–L140.

Radu, M., Chernoff, J., 2013. An in vivo assay to test blood vessel permeability. JoVE 73, e50062.

Scott, M.L., Fujita, T., Liou, H.C., Nolan, G.P., Baltimore, D., 1993. The P65 subunit of NF-kappa B regulates I kappa B by two distinct mechanisms. Genes Dev. 7, 1266–1276.

Shichijo, M., Sugimoto, H., Nagao, K., Inbe, H., Encinas, J.A., Takeshita, K., Bacon, K.B., Gantner, F., 2003. Chemoattractant receptor-homologous molecule expressed on Th2 cells activation in vivo increases blood leukocyte counts and its blockade abrogates 13, 14-dihydro-15-keto-prostaglandin D2-induced eosinophilia in rats. J. Pharmacol. Exp. Ther. 307, 518–525.

Singer, M., Sansonetti, P.J., 2004. IL-8 is a key chemokine regulating neutrophil recruitment in a new mouse model of Shigella-induced colitis. J. Immunol. 173, 4197–4206.

Singh, D., Cadden, P., Hunter, M., Collins, L.P., Perkins, M., Pettipher, R., Townsend, E., Vinall, S., O'Connor, B., 2013. Inhibition of the asthmatic allergen challenge response by the CRTH2 antagonist OC000459. Eur. Respir. J. 41, 46–52.

Stebbins, K.J., Broadhead, A.R., Correa, L.D., Scott, J.M., Truong, Y.P., Stearns, B.A., Hutchinson, J.H., Prasit, P., Evans, J.F., Lorrain, D.S., 2010. Therapeutic efficacy of AM156, a novel prostanoid DP 2 receptor antagonist, in murine models of allergic rhinitis and house dust mite-induced pulmonary inflammation. Eur. J. Pharmacol. 638, 142–149.

Straumann, A., Hoesli, S., Bussmann, C., Stuck, M., Perkins, M., Collins, L., Payton, M., Pettipher, R., Hunter, M., Steiner, J., 2013. Anti-eosinophil activity and clinical efficacy of the CRTH2 antagonist OC000459 in eosinophilic esophagitis. Allergy 68, 375–385.

Strieter, R.M., Kunkel, S.L., 1994. Acute lung injury: the role of cytokines in the elicitation of neutrophils. J. Investig. Med. 42, 640–651.

Suzuki, S., Ishii, M., Asami, T., Namkoong, H., Yagi, K., Asakura, T., Kamata, H., Tasaka, S., Kagawa, S., Kamo, T., 2016. Critical role of the prostaglandin D_2 receptor CRTH2 in acute lung injury caused by lipopolysaccharide (LPS)-induced shock in mice, C105. Respiratory Failure: mechanistic Insights from Lung Injury Models. Am. Thoracic. Soc. 193 A6285.

Tajima, T., Murata, T., Aritake, K., Urade, Y., Hirai, H., Nakamura, M., Ozaki, H., Hori, M., 2008. Lipopolysaccharide induces macrophage migration via prostaglandin D_2 and prostaglandin E_2. J. Pharmacol. Exp. Ther. 326, 493–501.

Wheeler, A.P., Bernard, G.R., 2007. Acute lung injury and the acute respiratory distress syndrome: a clinical review. Lancet 369, 1553–1564.

Xu, C., Zou, C., Hussain, M., Shi, W., Shao, Y., Jiang, Z., Wu, X., Lu, M., Wu, J., Xie, Q., 2018. High expression of Sonic hedgehog in allergic airway epithelia contributes to goblet cell metaplasia. Mucosal Immunol. 11, 1306–1315.

Xu, M., Cao, F., Liu, L., Zhang, B., Wang, Y., Dong, H., Cui, Y., Dong, M., Xu, D., Liu, Y., 2011. Tanshinone IIA–induced attenuation of lung injury in endotoxemic mice is associated with reduction of hypoxia-inducible factor 1α expression. Am. J. Respir. Cell Mol. Biol. 45, 1028–1035.

Xu, X., Xie, Q., Shen, Y., Jiang, J., Chen, Y., Yao, H., Zhou, J., 2008. Mannose prevents lipopolysaccharide-induced acute lung injury in rats. Inflamm. Res. 57, 104–110.

Yang, R., Yang, L., Shen, X., Cheng, W., Zhao, B., Ali, K.H., Qian, Z., Ji, H., 2012. Suppression of NF-κB pathway by crocetin contributes to attenuation of lipopolysaccharide-induced acute lung injury in mice. Eur. J. Pharmacol. 674, 391–396.

Yang, S., Yu, Z., Wang, L., Yuan, T., Wang, X., Zhang, X., Wang, J., Lv, Y., Du, G., 2017. The natural product bergenin ameliorates lipopolysaccharide-induced acute lung injury by inhibiting NF-kappaB activition. J. Ethnopharmacol. 200, 147–155.

Yao, H.Y., Chen, L., Xu, C., Wang, J., Chen, J., Xie, Q.M., Wu, X., Yan, X.F., 2011. Inhibition of Rac activity alleviates lipopolysaccharide-induced acute pulmonary injury in mice. BBA Gen. Subj. 1810, 666–674.

Yu, P.J., Li, J.R., Zhu, Z.G., Kong, H.-Y., Jin, H., Zhang, J.Y., Tian, Y.X., Li, Z.-H., Wu, X.Y., Zhang, J.J., 2013. Praeruptorin D and E attenuate lipopolysaccharide/hydrochloric acid induced acute lung injury in mice. Eur. J. Pharmacol. 710, 39–48.

Zhang, Z., Luo, Z., Bi, A., Yang, W., An, W., Dong, X., Chen, R., Yang, S., Tang, H., Han, X., 2017. Compound edaravone alleviates lipopolysaccharide (LPS)-induced acute lung injury in mice. Eur. J. Pharmacol. 811, 1–11.

Zhou, X., Dai, Q., Huang, X., 2011. Neutrophils in acute lung injury. Front. Biosci. 17, 2278–2283.